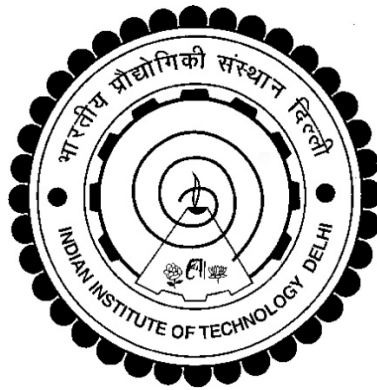


EXPERIMENTAL INVESTIGATION AND CFD
(VOF MODEL) VALIDATION OF INVERT TRAP
EFFICIENCY IN OPEN RECTANGULAR
CHANNEL

MOHD. MOHSIN



DEPARTMENT OF CIVIL ENGINEERING
INDIAN INSTITUTE OF TECHNOLOGY DELHI

August, 2017

© Indian Institute of Technology Delhi (IITD), New Delhi, 2017

EXPERIMENTAL INVESTIGATION AND CFD
(VOF MODEL) VALIDATION OF INVERT TRAP
EFFICIENCY IN OPEN RECTANGULAR
CHANNEL

by

MOHD. MOHSIN

Department of Civil Engineering

Submitted

in fulfillment of the requirements for the degree of Doctor of Philosophy

to the



Indian Institute of Technology Delhi

August, 2017

Certificate

This is to certify that the thesis entitled “**Experimental Investigation and CFD (VOF Model) Validation of Invert Trap Efficiency in Open Rectangular Channel**”, being submitted by **Mr. Mohd. Mohsin** to the Indian Institute of Technology, Delhi (India) for the award of the degree of **Doctor of Philosophy** in Civil Engineering, is a bonafide research work carried out by him under my supervision and guidance. The thesis, in my opinion, has reached the standard of fulfilling the requirement for the award of Doctor of Philosophy degree. The research report and the results presented in this thesis have not been submitted in parts or in full to any other University or Institute for the award of any degree or diploma.

August, 2017

(Dr. Deo Raj Kaushal)

(Supervisor)

Professor

Department Of Civil Engineering

Indian Institute of Technology Delhi

New Delhi-110016

Acknowledgements

First of all, I am highly grateful to Almighty God (Allah), The Most Beneficent, Gracious and Merciful, for blessing me motivation, courage and strength to complete and present this research work.

I express my deep sense of gratitude to my supervisor, Dr. D. R. Kaushal, for his invaluable continuous guidance and suggestions throughout the research work. He introduced me FLUENT, the “magic” world of numerical simulations of fluid flow. I am deeply indebted to him for his encouragement, motivation, co-operation and help without which this research work was not possible.

I extend my thanks to Prof. Manoj Datta, Head, Civil Engineering Department and members of my SRC, Prof. J. T. Shahu, Dr. C. T. Dhanya of Department of Civil Engineering and Dr. S. K. Pattanayek of Department of Chemical Engineering (member expert outside department) for their valuable suggestions and sparing their valuable time.

I deeply express my whole hearted feelings to my parents, brothers and sisters for their continuous encouragement and loving support. Deep sense of gratitude goes to my wife, Roshni, who suffered a lot during my absence but managed herself and strongly supported me, and two sons namely Raza and Zaki living at Aligarh and missing me during my Ph.D. I also acknowledge the good wishes and moral support from my mother in-law & brother in-law Er. M. A. Raza (Teepu).

I am very much thankful for the moral and encouraging support provided by my friends Satish Kumar, Basant Yadav, Nitesh Patidar, Gopinadh Rongali and all my remaining friends of Simulation Lab.

I am highly thankful to Prof. M. Jamil (Retired), Prof. Mubeen Beg, Prof. Javed Alam and Prof. Kausar Ali of Civil Engineering Department, Aligarh Muslim University, for their continuous moral support and encouragement.

I would also like to extend my thanks to Mr. N. R. Gehlot and Mr. Yaad Ram who were always ready for help in Simulation Laboratory of Water Resource Engineering. Sincere thanks to the staff of the Civil Engineering Department especially Mr. Rajveer Agrawal and Mr. Randheer for helping me for any official work. Everyone else who has helped me throughout the period of my research work also deserves a big thank. Special thanks must go to all my well-wishers who helped me directly or indirectly during my research work.

At the last, but not the least, I am thankful to Er. Osama M. Khan, Aligarh, for fabricating the Sediment Injector, Point Gauge and lids for my experimental work.

August, 2017

(Mohd. Mohsin)

Abstract

In modern times, due to rapid urbanization, the quantity of waste water going into the urban sewer systems has been increased significantly. The urban waste water includes construction debris, industrial wastes, natural sediments, urban solid wastes, wastes from roads etc. Sediment entrainment into the sewers or storm water drainage channels from the adjoining catchment areas, subsequently their movement and deposition in the channel reduce the flow area, and as a result the hydraulic efficiency of the channels gets reduced. Sediments get deposited on the invert (bottom) along the reach of the drainage channels during the period of dry weather due to non-availability of sufficient flow velocity which leads to the sedimentation and reduction in the carrying capacity of the channel. The water containing sediments creates environmental pollution and hinders the operation of pumps in Sewage Treatment Plants (STP) and turbines in Hydro Power Plants. It also adversely affects the aquatic and plant life in a river. Continuous efforts had been made by the mankind to understand the mechanics of movement of the sediments in running water. To solve the sediment problem in a flowing channel, sediment ejectors, excluders, extractors and a number of sediment trapping devices have been developed and are being used at suitable places along the reach of the channel to minimize the sediment content in the channel to ensure smooth and optimum functioning of the drainage system. Invert trap is one of the trapping device to trap the sediments flowing into a sewer or storm water drainage channel. As the name itself indicates, it is a chamber provided at the invert of the channel in which the sediment falls and gets trapped. Among sediment trapping structures, invert traps are very effective method of reducing the amount of sediment flowing in a drainage system and irrigation channels (Gupta et al. 2005).

Experimentation is required to analyze the effect of variable parameters of flow, trap geometry and sediments on the trap efficiency of an invert trap for its design and performance purpose. As experimentation is always not possible, time consuming or becomes a costly affair, Computational Fluid Dynamics (CFD) has now become an excellent and economically less expensive tool for the study of flow in sewers or storm water drainage systems. For the CFD modeling of invert traps in open channels, earlier investigators used Fixed Lid Model (FLM), i.e. assuming open channel flow as closed conduit flow with top wall as shear free wall, with stochastic Discrete Phase Model (DPM). This approximate model was poorly validated with their experimental data. In the present study, experimentation has shown that the free water surface rises above the central slot (opening) of the invert trap which can not be modelled using FLM because water surface fluctuations/profiles are not possible in closed conduits. Therefore, in the present study without making such assumptions, the appropriate Computational Fluid Dynamics (CFD) model for open channel flow i.e. Volume of Fluid (VOF) model along with stochastic DPM has been used. This VOF model has been extensively validated with the experimental results in which only natural sediments including actual sewer solids have been used. 2D & 3D CFD analysis show that 2D predicts a little lower trap efficiencies than 3D which is theoretically as well as experimentally justified because in 3D modeling, more sediments fall into the trap due to their low velocity near the walls (which has also been observed experimentally) and subsequently giving higher values of trap efficiency which is contrary to the presumption of [Buxton et al. \(2002\)](#) that the 3D may predict low values. The CFD predicted Water Surface Profile (WSP) above the central opening (slot) of the invert trap has also been compared and validated with the experimentally measured WSP. In addition, the CFD predicted flow field has been satisfactorily compared with the experimentally measured velocities using Laser Particle Image Velocimetry (PIV). On the basis of the present study, it can be concluded VOF

model along with stochastic DPM is the appropriate CFD model in comparison to FLM for the numerical performance and design analysis of invert traps. It has also been established that 2D predicts the same qualitative results as 3D but quantitatively, 3D model predicts the best results in comparison to the experimental results.

सार (सारांश)

आधुनिक समय में, तेजी से शहरीकरण के कारण, शहरी सीवर सिस्टम में जा रहे तलछट (सेडिमेन्ट्स) की मात्रा में काफी वृद्धि हुई है। शहरी अपशिष्ट जल (वेस्ट वॉटर) में निर्माण का मलबा, औद्योगिक अपशिष्ट, प्राकृतिक तलछट, शहरी ठोस अपशिष्ट तथा सड़कों के अपशिष्ट आदि शामिल हैं। आस-पास के जलग्रहण क्षेत्रों से बारिश के जल निकासी चैनलों में तलछट के प्रवेश और इसके बाद उनके चैनल में जमा होने से जल प्रवाह क्षेत्र कम हो जाता है, और परिणामस्वरूप चैनलों की हाइड्रोलिक दक्षता (एफिशिएंसी) कम हो जाती है। पर्याप्त जल प्रवाह वेग की अनुपलब्धता के चलते सूखे मौसम (ड्राइ वेदर) की अवधि के दौरान जल निकासी चैनलों में तलछट (सेडिमेन्ट्स) नीचे (बाटम अथवा पेंदी में) जमा हो जाता है जिससे चैनलों की क्षमता और अवसादन में कमी आ जाती है। तलछट युक्त पानी पर्यावरण में प्रदूषण और सीवेज ट्रीटमेंट प्लांट्स (एसटीपी) में पंपों और हाइड्रो पावर प्लांट्स में टर्बाइनों के संचालन में बाधा उत्पन्न करता है। यह (सेडिमेन्ट्स) नदी में जलीय जीवों और पौधों को प्रतिकूल रूप से प्रभावित करता है। पानी में तलछटों के प्रवाह की यांत्रिकी को समझने के लिए मानव जाति द्वारा निरंतर प्रयास किए गए हैं। जल प्रवाह चैनलों में तलछट की समस्या को हल करने के लिए तलछट के अपवर्जन, एक्स्ट्रेक्टर और अनेक प्रकार के तलछट फंसाने वाले उपकरणों को विकसित किया गया है, जिनको चैनलों में उपयुक्त स्थानों पर उपयोग किया जा रहा है ताकि चैनलों में तलछट सामग्री को कम किया जा सके और यह सुनिश्चित हो सके कि जल निकासी प्रणाली उचित प्रकार से कार्य कर रही है। इन्वर्ट ट्रेप सीवर या बरसाती जल निकासी चैनल में बहने वाले तलछटों को फंसाने वाला एक प्रकार का उपकरण है। जैसा कि नाम से ही इंगित है कि यह एक चैम्बर है जो कि चैनल के तल (इन्वर्ट या बाटम) पर प्रदान किया जाता है। चैनल में बहता हुआ तलछट इन्वर्ट ट्रेप में गिर कर फंस जाता है। तलछट फँसाने वाली संरचनाओं में इन्वर्ट ट्रेप जल निकासी प्रणाली और सिंचाई

चैनल (नहर) में बहने वाले तलछटों की मात्रा को कम करने का बहुत प्रभावी तरीका है (गुप्ता व अन्य, 2005)।

इसके डिजाइन और प्रदर्शन के उद्देश्य में इन्वर्ट ट्रेप की दक्षता पर जल प्रवाह की तीव्रता, इन्वर्ट ट्रेप की ज्यामिति और तलछट के चर (वैरिएबल) पैरामीटर के प्रभाव का विश्लेषण करने के लिए प्रयोग की आवश्यकता होती है। जैसा कि प्रयोग हमेशा संभव नहीं होता है, समय लगता है अथवा आर्थिक रूप से महंगा मामला बन जाता है, कम्प्यूटेशनल फ्लूइड डायनेमिक्स (सीएफडी) अब गंदे पानी की नाली (सूअज चैनल) या बरसाती जल निकासी व्यवस्था में जल प्रवाह के अध्ययन के लिए एक उत्कृष्ट और आर्थिक रूप से कम महंगा उपकरण अथवा साधन बन गया है। पहले के जांचकर्ताओं ने खुले चैनलों में इन्वर्ट ट्रेप की सीएफडी मॉडलिंग के लिए फिक्स्ड लिड मॉडल (एफएलएम अर्थात खुले चैनल प्रवाह को बंद पाइपलाइन प्रवाह, अथवा क्लोज्ड कान्डूइड फ्लो, के रूप में ऊपर की दीवार (छत) को शियर मुक्त (शियर फ्री) मानते हुए) के साथ स्टोकेस्टिक पृथक चरण मॉडल (डीपीएम – डिस्क्रीट फेज़ मॉडल) का इस्तेमाल किया था। यह अनुमानित मॉडल उनके प्रयोगात्मक डेटा के साथ संतोषजनक रूप से मान्य नहीं हो पाया था। वर्तमान अध्ययन में, प्रयोग से पता चला है कि पानी की सतह इन्वर्ट ट्रेप के केंद्रीय स्लॉट के ऊपर बढ़ जाती है, जिसे एफएलएम के द्वारा मॉडल नहीं किया जा सकता क्योंकि पानी की सतह में उतार चढ़ाव क्लोज्ड कान्डूइड फ्लो में संभव नहीं हैं। इसलिए, इस तरह की धारणाएं किए बिना, वर्तमान अध्ययन में खुले चैनल प्रवाह के लिए उपयुक्त कम्प्यूटेशनल फ्लूइड डायनेमिक्स (सीएफडी) मॉडल, स्टोकेस्टिक (प्रसंभाव्य) डीपीएम के साथ वॉल्यूम आफ फ्लूइड (वीओएफ) मॉडल का इस्तेमाल किया गया है। इस वीओएफ मॉडल को प्रायोगिक परिणामों के साथ बड़े पैमाने पर मान्य किया गया है जिसमें वास्तविक सीवर में बहने वाले ठोस पदार्थों सहित केवल प्राकृतिक तलछट (अवसाद) का उपयोग किया गया है। 2 डी (दो आयामी) और 3 डी (तीन आयामी) सीएफडी विश्लेषण बताते हैं कि 2 डी 3 डी की तुलना में थोड़ा कम इन्वर्ट ट्रेप की दक्षता की भविष्यवाणी करता है, जो कि सैद्धांतिक और प्रयोगात्मक रूप से उचित

है, क्योंकि 3 डी मॉडलिंग में, चैनल की दीवारों के निकट वाले बहने वाले तलछट, पानी के कम वेग के कारण, अधिक मात्रा में इन्वर्ट ट्रेप में गिरते हैं (जो कि प्रयोगात्मक रूप से भी देखा गया है) और परिणाम स्वरूप जाल दक्षता (ट्रेप इफिशियन्सी) की उच्च मात्रा की भविष्यवाणी होती है, जो कि बक्सटन व अन्य (2002) के अनुमान के विपरीत है कि 3 डी मॉडल जाल दक्षता की कम मात्रा की भविष्यवाणी कर सकते हैं। केंद्रीय स्लॉट के ऊपर पानी की सतह (डब्ल्यूएसपी-वॉटर सरफेस प्रोफाइल) की सीएफडी द्वारा भविष्यवाणी की भी तुलना प्रयोगात्मक रूप से मापी गई पानी की सतह से की गई है। इसके अलावा, सीएफडी द्वारा अनुमानित प्रवाह क्षेत्र की लेजर कण छवि वेलोसिमेट्री (पीआईवी-पार्टिकल इमिज वेलोसिमेट्री) का उपयोग करते हुए प्रयोगात्मक रूप से मापे गए वेगों (वेलोसिटी या गति) के साथ संतोषजनक ढंग से तुलना की गई है। वर्तमान अध्ययन के आधार पर, यह निष्कर्ष निकाला जा सकता है कि स्टोकेस्टिक (प्रसंभाव्य) डीपीएम के साथ वॉल्यूम आफ फ्लूइड (वीओएफ) मॉडल एफएलएम की तुलना में इन्वर्ट ट्रेप के सांख्यिकीय प्रदर्शन और डिजाइन विश्लेषण के लिए यह एक उपयुक्त सीएफडी मॉडल है। यह भी स्थापित किया गया है कि 2 डी मॉडल 3 डी मॉडल के मुकाबले में एक ही गुणात्मक परिणामों की भविष्यवाणी करता है, लेकिन मात्रात्मक रूप से, 3 डी मॉडल प्रायोगिक परिणामों के मुकाबले सबसे अच्छे (उच्चतम) परिणाम की भविष्यवाणी करता है।

Contents

Certificate	i
Acknowledgements	iii
Abstract	v
Contents	ix
List of Figures	xv
List of Tables	xix
Chapter 1 Introduction	1
1.1 Sediment	4
1.2 Sedimentation	5
1.3 Hydraulic Transportation of Solids in Open Channels	5
1.3.1 Preventive Measures	6
1.3.2 Curative Measures	7
1.4 Invert Trap	7
1.5 Trap Efficiency (η)	8
1.6 Computational Fluid Dynamics (CFD) Modeling	9
1.7 Published Experimental and CFD Work on Invert Trap	9
1.8 Research Gap	12
1.9 Objectives of the Present Study	12
1.10 Research Program	14
1.11 Scope of the Present Work	14
1.12 Organization of the Thesis	16
Chapter 2 Literature Review	19
2.1 Sediment Transportation	46
2.1.1 Origin and Properties of Sediments	46
2.1.2 Mineral Composition	50
2.1.3 Surface Texture	50
2.1.4 Bulk Properties of Sediments	50
2.1.5 Incipient Motion of Sediment Particles	52
2.1.6 Regimes of Flow	53
2.2 Bed Load Transport and Saltation	56
2.3 Bed Load Equations	58
2.4 Mechanism of Saltation	59
2.5 Suspended Load Transport	60
2.6 Mechanism of Suspension	61
2.7 Suspended Load Equations	61

2.8	Wash Load	62
2.9	Sewer Flushing	64
2.10	Grit Chambers	65
2.11	Invert/Silt/Bed Load Traps	66
2.12	Sediment in Urban Drainage System	71
2.13	Causes & Impacts of Sewer Sediment	72
2.13.1	Hydraulic Design of Combined Sewers	72
2.13.2	Re-entrainment of Settled Sediments	72
2.13.3	Structural Disintegration & Odour Problems	72
2.13.4	Biological Impacts	73
2.14	Sewer Sediment Control	73
2.14.1	Integrated Approach	74
2.14.2	Physical or Conventional Sewer Cleaning Techniques	75
2.14.3	Sewer Cleaning by Flushing	77
Chapter 3	CFD (VOF Model) Theory	81
3.1	Major Assumptions	81
3.2	CFD Model for Two-Phase (Liquid-Gas) Flows	81
3.3	Euler-Euler Approach	82
3.4	Volume of Fluid (VOF) Model	82
3.4.1	Continuity Equation (Volume Fraction Equation)	84
3.4.2	Momentum Equation	85
3.4.3	Open Channel Flow	86
3.4.4	Pressure-implicit with Splitting of Operators (PISO)	87
3.5	Discrete Phase Model (DPM)	88
3.5.1	Discrete Phase-Particle Tracking	88
3.5.2	Drag Coefficient of Sphere (C_D)	89
3.5.3	Particle trajectories	89
3.5.4	Drag Law	90
3.5.5	Integral Time	90
3.6	CFD Model Setup	91
3.6.1	Two-way Coupling	91
3.6.2	Turbulence Models	92
3.6.3	Non-equilibrium Wall Functions	93
3.6.4	Surface Tension and Wall Adhesion	94
3.7	Grid (Mesh) Generation	94
3.7.1	Cell (Grid) Quality	95
Chapter 4	Case Studies	97
4.1	Case Study-I	97
4.1.1	Abstract	97
4.1.2	Present Case Study	98
4.2	Case Study-II	116

4.2.1	Abstract	116
4.2.2	Present Case Study	117
4.2.3	Data and Methods	117
4.3	Case Study-III	129
4.3.1	Abstract	129
4.3.2	Present Case Study	130
Chapter 5	Experimental Investigation	149
5.1	Laboratory Apparatus	149
5.1.1	Inlet Tank	152
5.1.2	Collecting Tank	152
5.1.3	Open Rectangular Channel	153
5.1.4	Invert Trap	153
5.1.5	Pump (2 HP)	154
5.1.6	Regulators	154
5.1.7	Sediment Injector or Sediment Feeder	154
5.1.8	Point Gauge	158
5.1.9	Bed Slope Device	158
5.2	Sediment Collecting System	159
5.3	Flow Depth-Velocity Relationship	160
5.4	Bed Shear Velocity	161
5.5	Sediment Particles	162
5.6	Sedimentation Parameter (S_p)	164
5.7	Physical Properties of the Sediments	165
5.7.1	Particle Size Distribution of Sewer Solid	165
5.7.2	Sieve Analysis	165
5.7.3	Specific Gravity of Sediments (G)	167
5.7.4	Fall (Settling) Velocity (ω_s)	167
5.7.5	Sedimentation Parameter Range	168
5.7.6	Summary of Sediment Characteristics	168
5.8	Definition of Trap Efficiency	169
5.9	Parametric Analysis	170
5.10	General Experimental Methodology	171
5.11	Sediment Transfer Time	173
5.12	Program of Experimental Tests	173
5.13	Experimental Test Results	174
5.14	Analysis of Results	180
5.14.1	Effect of Discharge Intensity (q) on Trap Efficiency (η)	180
5.14.2	Effect of Slot Size (Δx) on Trap Efficiency (η)	182
5.14.3	Effect of Sedimentation Parameter (S_p) on Trap Efficiency (η)	185
5.14.4	Sediment Particle Deposition Profile Inside the Trap	189
5.15	Performance Parameters	193

Chapter 6	2D CFD (VOF) Modeling	195
6.1	2D CFD Modeling of the Invert Trap	196
6.1.1	Geometry for the 2D CFD Model Setup	197
6.1.2	Grid Generation	197
6.1.3	Flow Field Input Parameter	199
6.1.4	Input Flow Parameter	199
6.1.5	Boundary Conditions	200
6.1.6	Solution Strategy and Convergence	200
6.1.7	Near-Wall Modeling	201
6.1.8	Input Model Parameters	202
6.1.9	Particle Tracking Input Parameters	202
6.1.10	Discrete Phase Boundary Condition	203
6.1.11	Time Scale Constant (C_L)	203
6.1.12	Injection Type and Injection Location	203
6.1.13	Particle Type, Diameter and Density	204
6.1.14	Initial Particle Velocities	204
6.1.15	Number of Stochastic Tries	205
6.1.16	Number of Discrete Time Steps	205
6.1.17	Length Scale	205
6.2	Result and Analysis	206
6.2.1	Trap Efficiency Prediction	216
6.2.2	Sediment Particle Tracking	218
Chapter 7	3D CFD (VOF) Modeling	219
7.1	3D CFD (VOF) Modeling	219
7.1.1	Geometry for the 3D CFD Model Setup	220
7.1.2	Grid Generation	221
7.1.3	Input Flow Parameter	222
7.1.4	Boundary Conditions	223
7.1.5	Solution Strategy and Convergence	223
7.1.6	Near-Wall Modeling	224
7.1.7	Input Parameters	224
7.1.8	Particle Tracking Input Parameters	224
7.1.9	Discrete Phase Boundary Condition	225
7.1.10	Time Scale Constant	225
7.1.11	Injection Type and Injection Location	225
7.1.12	Particle Type, Diameter and Density	225
7.1.13	Initial Particle Velocities	225
7.1.14	Number of Stochastic Tries	226
7.1.15	Number of Discrete Time Steps	227
7.2	Result and Analysis	227
7.2.1	Flow Field	233
7.2.2	Validation of Water Surface Profile	235
7.2.3	Variation in Turbulent Kinetic Energy	237

	7.2.4 Trap Efficiency Prediction	238
Chapter 8	Comparison of Results	243
8.1	Comparison of Trap Efficiencies	243
8.2	Graphical Comparison of η	250
Chapter 9	Validation of CFD Flow Field with PIV	255
9.1	Laser PIV System	255
9.1.1	Introduction	255
9.1.2	Precautions	256
9.1.3	Seeding	256
9.1.4	The rtCam	257
9.1.5	The nanoLase	257
9.1.6	rtControl Software	258
9.2	Experimentation Process	258
9.2.1	Installation of the Software	258
9.2.2	Connecting the Hardware	259
9.2.3	Seeding	259
9.2.4	Start the rtControl	259
9.2.5	Setting the rtCam and nanoLase	260
9.2.6	Generation of Vectors	261
9.2.7	Recording an Image Sequence	261
9.2.8	Reviewing of Saved Data	262
9.3	Experimentation with PIV	263
9.3.1	Measurements in Rectangular Channel	263
9.3.2	Measurements inside the Invert Trap	266
Chapter 10	Conclusions and Scope for Future Work	269
10.1	Conclusions	269
10.2	Scope for Future Work	271
Appendix-I	Publications from Present Research Work	273
Appendix-II	List of Symbols	275
Appendix-III	List of Abbreviations	279
References		281
Brief Bio-data		299

List of Figures

Fig. 1.1 Waste water system chain	1
Fig. 1.2 Photo view of the sediments in sewer	2
Fig. 1.3 Photo view of the sediments entering into storm water drainage systems	3
Fig. 1.4 Types of invert trap	7
Fig. 1.5 Potential storm water particulate trap	10
Fig. 1.6 Frame work of the research program	14
Fig. 2.1 Different shapes of the sediments	47
Fig. 2.2 Chart showing the sediment classification on the basis of their size	48
Fig. 2.3 Types of bed forms in alluvial channels	56
Fig. 2.4 Processes of erosion, transport and sedimentation (Julien, 2010)	57
Fig. 2.5 Definition sketch of the bed & suspended load layer (Julien, 2010)	58
Fig. 2.6(a) Four idealized position of saltating particles (b) Forces acting on a saltating particle in position 2. (Garde & Raju, 2000)	60
Fig. 2.7 Flushing system for an open channel	65
Fig. 2.8 Traditional French grit chamber (Ashley et al., 2004)	66
Fig. 2.9 Invert trap (Ashley et al. 2004)	67
Fig. 2.10 Diagram showing the operation of a hydrass gate	78
Fig. 2.11 Flushing gate (Pisano et al. 2003)	79
Fig. 2.12 Hydrosel self wave flush in trunk sewers	80
Fig. 3.1 Schematic diagram showing the present CFD approach	84
Fig. 4.1 The 2D-Rectangular channel fitted with invert trap	99
Fig. 4.2 2D-Rectangular channel fitted with invert trap showing quadrilateral mesh	100
Fig. 4.3 y^+ vales for the u/s bed	104
Fig. 4.4 y^+ vales for the d/s bed	105
Fig. 4.5 Volume fraction of water and air ($\Delta x = 15$ cm, $U = 0.7$ m.s ⁻¹ , $d = 1.5$ cm)	106
Fig. 4.6 Velocity vectors colored by volume fraction of water	107
Fig. 4.7 Velocity contours colored by velocity magnitude	107
Fig. 4.8 Velocity vectors colored by volume fraction of water	107
Fig. 4.9 Velocity contours colored by velocity magnitude	107
Fig. 4.10 Velocity vectors colored by volume fraction of water	108
Fig. 4.11 Velocity contours colored by velocity magnitude	108
Fig. 4.12 Contours of static pressure of mixture in Pa	108
Fig. 4.13 Particle trajectories colored by particle ID	108
Fig. 4.14 Contours of static pressure of mixture in Pa	108
Fig. 4.15 Particle trajectories colored by particle ID	108
Fig. 4.16 Contours of static pressure of mixture in Pa	109
Fig. 4.17 Particle trajectories colored by particle ID	109
Fig. 4.18 Velocity contours colored by velocity magnitude	109

Fig. 4.19	Velocity contours colored by velocity magnitude	109
Fig. 4.20	Variation of η with Δx for $U = 0.9 \text{ m.s}^{-1}$, $d = 2.5 \text{ cm}$ (sand0.15)	113
Fig. 4.21	Variation of η with Δx for $U = 0.7 \text{ m.s}^{-1}$, $d = 1.5 \text{ cm}$ (glassbead0.3)	113
Fig. 4.22	Experimental versus predicted trap efficiency (glassbead0.3)	114
Fig. 4.23	3D Rectangular channel fitted with an invert trap	118
Fig. 4.24	3D Rectangular channel fitted with invert trap meshed with 584485 tetrahedral cells	118
Fig. 4.25	Distribution of velocity contours for $\Delta x = 9 \text{ cm}$, $U = 1.0 \text{ m.s}^{-1}$ and $d = 3.0 \text{ cm}$	122
Fig. 4.26	Velocity vectors at central plane colored by volume fraction of water for $\Delta x = 9 \text{ cm}$, $U = 0.7 \text{ m.s}^{-1}$ and $d = 1.5 \text{ cm}$	123
Fig. 4.27	Velocity contours at central plane for $\Delta x = 9 \text{ cm}$, $U = 0.7 \text{ m.s}^{-1}$ and $d = 1.5 \text{ cm}$	123
Fig. 4.28	Contours of static pressure at central plane for $\Delta x = 9 \text{ cm}$, $U = 1.0 \text{ m.s}^{-1}$ and $d =$ 3.0 cm	124
Fig. 4.29	Particle trajectory by means of particle number for $\Delta x = 9 \text{ cm}$, $U = 1.0 \text{ m.s}^{-1}$	124
Fig. 4.30	Contours of volume fraction of water and air for $\Delta x = 9 \text{ cm}$, $U = 1.0 \text{ m.s}^{-1}$ and $d =$ 3.0 cm	124
Fig. 4.31	Trap Efficiency for flow velocity of 0.7 m.s^{-1} and depth of flow of 1.5 cm	127
Fig. 4.32	Experimental versus predicted trap efficiency	127
Fig. 4.33	Dimensions of the trapezoidal channel with rectangular trap	131
Fig. 4.34	X-section of the trapezoidal channel	131
Fig. 4.35	Isometric view of discretized geometry using hexahedral mesh for 3D-CFD analysis (29, 84,800 meshes, M3 model)	134
Fig. 4.36	Volume fraction of water and air at the central plane	134
Fig. 4.37	Velocity contours at the central plane, trap bottom & d/s vertical wall (M2)	137
Fig. 4.38	Velocity vectors at the central plane (M2 model)	137
Fig. 4.39	Top view of free water surface profile (M2)	138
Fig. 4.40	Contours of static pressure at the central plane (M2 model)	139
Fig. 4.41	The ‘incomplete’ particles inside the trap and treated as trapped particles after stopping the flow	141
Fig. 4.42	Comparison of predicted retention efficiency with particle diameter of sand	142
Fig. 4.43	Possible particle trajectories (M1)	143
Fig. 4.44	Particle traces during trapping and escaping (M1)	144
Fig. 4.45	Variation of retention efficiency with sedimentation parameter (Figure 7: Buxton et al., 2002)	146
Fig. 5.1	The plan and elevation of the experimental set-up	150
Fig. 5.2	Pictorial view of the experimental setup at Water Resource Laboratory Deptt. of Civil Engg., IIT Delhi	151
Fig. 5.3	Cross-sectional view of the rectangular channel fitted with the invert trap	151
Fig. 5.4	The invert trap geometry selected for the investigation	154
Fig. 5.5	Drawing of the proposed sediment injector	155
Fig. 5.6	Plan and section of the proposed sediment injector	156

Fig. 5.7 Pictorial view of the gravity-operated sediment injector	157
Fig. 5.8 Fabricated point gauge for measuring the depth of flow	158
Fig. 5.9 Close pictorial view of the bed slope device	159
Fig. 5.10 Flow depth-velocity relationship for the laboratory channel	160
Fig. 5.11 Bed shear velocity versus depth of flow	161
Fig. 5.12 Particle size distribution of the field sewer solids collected	167
Fig. 5.13 Collected trapped sediments from invert trap on a 75 μm sieve and ready for oven drying	172
Fig. 5.14 The variation of η with discharge intensity, SS, $\Delta x = 15$ cm	181
Fig. 5.15 The variation of η with discharge intensity, CS, $\Delta x = 15$ cm	182
Fig. 5.16 The variation of η with discharge intensity, BA, $\Delta x = 15$ cm	182
Fig. 5.17 Variation of η with slot size, Δx	183
Fig. 5.18 Variation of η with slot size, Δx	183
Fig. 5.19 Variation of η with slot size, Δx	184
Fig. 5.20 Variation of η with s_p for $\Delta x = 15$ cm	185
Fig. 5.21 Variation of η with s_p for $\Delta x = 12$ cm	186
Fig. 5.22 Variation of η with s_p for $\Delta x = 9$ cm	187
Fig. 5.23 Variation of η with s_p for varying Δx	188
Fig. 5.24 Particle passing straight over the trap	189
Fig. 5.25 Particle re-entraining back into the main flow	190
Fig. 5.26 Particle settles into the trap	190
Fig. 5.27 Particle settles into the trap	191
Fig. 5.28 Particle deposition profile inside the trap	192
Fig. 6.1 2D view of the rectangular channel fitted with an invert trap	197
Fig. 6.2 2D Meshing of rectangular channel with invert trap (Quadrilateral mesh)	198
Fig. 6.3 Channel with water and air fraction (d5x9 model)	213
Fig. 6.4 Mass balance monitor at inlet and outlet (d1x15 model)	213
Fig. 6.5 Velocity contours ($d = 5$ cm, $\Delta x = 9$ cm, 2D)	214
Fig. 6.6 Velocity vectors ($d = 5$ cm, $\Delta x = 15$ cm, 2D)	215
Fig. 6.7 Variation of turbulent kinetic energy inside the trap (d2x3)	215
Fig. 6.8 Variation of trap efficiency with slot size	216
Fig. 6.9 Variation of trap efficiency with diameter of the particle	217
Fig. 6.10 Relation between retention ratio and sedimentation parameter	217
Fig. 6.11 The particle trajectory inside the trap (d5x15, SS2)	218
Fig. 6.12 Incomplete particles in equilibrium with flow (d5x15, SS2)	218
Fig. 7.1 3D view of laboratory channel with invert trap	221
Fig. 7.2 Isometric view of discretized geometry using hexahedral cell (12,89,112 meshes of 4 mm size for $d = 5$ cm)	222
Fig. 7.3 Channel with water and air fraction ($d = 5$ cm, $\Delta x = 9$ cm, 3D)	234
Fig. 7.4 Velocity contours at mid plane ($d = 5$ cm, $\Delta x = 15$ cm, 3D)	234
Fig. 7.5 Velocity vectors at mid plane ($d = 5$ cm, $\Delta x = 15$ cm, 3D)	235

Fig. 7.6 Comparison of experimental and VOF predicted water surface profile at mid plane(D2X12)	236
Fig. 7.7 The turbulent kinetic energy at the central plane and inside the trap	237
Fig. 7.8 Path followed by the particle inside the trap	239
Fig. 7.9 Particle position as simulated and observed experimentally	240
Fig. 7.10 Trap efficiency versus slot size for SS1	241
Fig. 7.11 Variation of trap efficiency with diameter of the particle	241
Fig. 7.12 Trap efficiency versus S_p plot for all sediments	242
Fig. 7.13 Comparison of experimental and 3D-CFD predicted trap efficiency	242
Fig. 8.1 Trap efficiency versus slot size for SS1	250
Fig. 8.2 Trap efficiency versus slot size for SS2	251
Fig. 8.3 Trap efficiency versus slot size for CS1	251
Fig. 8.4 Trap efficiency versus slot size for CS2	252
Fig. 8.5 Trap efficiency versus slot size for CS3	252
Fig. 8.6 Trap efficiency versus slot size for BA	253
Fig. 9.1 The rtCam and nanoLase	258
Fig. 9.2 Position of rtCam and nanoLase	260
Fig. 9.3 Recording and display setting	262
Fig. 9.4 Photo view during PIV measurements	263
Fig. 9.5 Velocity vectors using PIV	264
Fig. 9.6 Comparison of velocity profile	265
Fig. 9.7 Comparison of 3D CFD predicted and PIV measured velocity profile	266
Fig. 9.8 Qualitative comparison of PIV and 3D CFD predicted velocity vectors at the bottom of the invert trap ($d = 5$ cm, $\Delta x = 15$ cm)	267

List of Tables

Table 4.1	2D-CFD model flow parameters (width, $b = 1.0$ m)	100
Table 4.2	Characteristics of sediments used	101
Table 4.3	CFD - VOF model setup with boundary conditions	101
Table 4.4	Mass flow rate of water	105
Table 4.5	DPM variable parameters setup	110
Table 4.6	Comparison of trap efficiencies (sand0.15)	111
Table 4.7	Comparison of trap efficiencies (glassbead0.3)	112
Table 4.8	Variable parameters for 3D-CFD modelling	118
Table 4.9	Comparison of predicted trap efficiency with the experimental data	126
Table 4.10	Inlet flow properties ($b = 0.14$ m, $z = 0.404206$, $S_o = 0.0015$)	132
Table 4.11	Sediments properties	132
Table 4.12	Mesh details used in the CFD (VOF) model analysis (Hexahedral cells)	133
Table 4.13	VOF model and DPM setup parameters	135
Table 4.14	Mass balance of water at convergence	136
Table 4.15	3D-CFD predicted trap efficiencies for M1 model	144
Table 4.16	3D-CFD predicted trap efficiencies for M2 model	145
Table 4.17	3D-CFD predicted trap efficiencies for M3 model	145
Table 5.1	Summary of channel parameters	162
Table 5.2	Flow properties of the channel	163
Table 5.3	Classification of sewer solids based upon sedimentation parameter	164
Table 5.4	Set of sieves used for PSD of sewer solids	166
Table 5.5	Calculation for plotting the PSD for sewer solids	166
Table 5.6	Summary of sediment particles	169
Table 5.7	Observation table for the experimental tests	173
Table 5.8	Laboratory results for sewer solid (SS1)	175
Table 5.9	Laboratory results for sewer solid (SS2)	176
Table 5.10	Laboratory results for commercial sand (CS1)	177
Table 5.11	Laboratory results for commercial sand (CS2)	178
Table 5.12	Laboratory results for commercial sand (CS3)	179
Table 5.13	Laboratory results for bottom ash (BA)	180
Table 5.14	Model performance parameter used in the present study	193
Table 6.1	Mesh details used in the 2D-CFD (VOF) model analysis	198
Table 6.2	Flow parameters for 2D-CFD modeling ($b = 1.0$ m, $S_o = 0.006$)	199
Table 6.3	Mass balance of water at convergence (for $d = 2$ cm, $\Delta x = 9$ cm)	201
Table 6.4	Summary of basic computational configuration parameters	202
Table 6.5	Input parameters for particle tracking	205
Table 6.6	Comparison of 2D predictions with experimental results for SS1	207
Table 6.7	Comparison of 2D predictions with experimental results for SS2	208
Table 6.8	Comparison of 2D predictions with experimental results for CS1	209

Table 6.9	Comparison of 2D predictions with experimental results for CS2	210
Table 6.10	Comparison of 2D predictions with experimental results for CS3	211
Table 6.11	Comparison of 2D predictions with experimental results for BA	212
Table 7.1	Mesh details used in the 3D CFD (VOF) model analysis	222
Table 7.2	Flow parameters for 3D-CFD modeling ($b = 0.15$ m, $S_o = 0.006$)	222
Table 7.3	Mass balance of water at convergence (for $d = 2$ cm, $\Delta x = 9$ cm)	223
Table 7.4	Effect of number of stochastic tries on trap efficiency	226
Table 7.5	Comparison of 3D predictions with experimental results for SS1	228
Table 7.6	Comparison of 3D predictions with experimental results for SS2	229
Table 7.7	Comparison of 3D predictions with experimental results for CS1	230
Table 7.8	Comparison of 3D predictions with experimental results for CS2	231
Table 7.9	Comparison of 3D predictions with experimental results for CS3	232
Table 7.10	Comparison of 3D predictions with experimental results for BA	233
Table 8.1	Comparison of 2D & 3D prediction with experimental results for SS1	244
Table 8.2	Comparison of 2D & 3D prediction with experimental results for SS2	245
Table 8.3	Comparison of 2D & 3D prediction with experimental results for CS1	246
Table 8.4	Comparison of 2D & 3D prediction with experimental results for CS2	247
Table 8.5	Comparison of 2D & 3D prediction with experimental results for CS3	248
Table 8.6	Comparison of 2D & 3D prediction with experimental results for BA	249
Table 9.1	Flow parameters in the channel flow	264
Table 9.2	Comparison of 3D CFD and PIV predicted velocity	265